Polymer Degradation and Stability 122 (2015) 8–17

Contents lists available at ScienceDirect

Polymer Degradation and Stability

journal homepage: www.elsevier.com/locate/polydegstab

Synthesis and characterization of aluminum poly-hexamethylenephosphinate and its flame-retardant application in epoxy resin

Jingyu Wang, Lijun Qian*, Bo Xu, Wang Xi, Xinxin Liu

Department of Materials Science & Engineering, Beijing Technology and Business University, Beijing 100048, PR China

ARTICLE INFO

Article history:
Received 21 August 2015
Received in revised form
9 October 2015
Accepted 11 October 2015
Available online 19 October 2015

Keywords:
Flame retardant
Phosphinate
Epoxy resin
Alkyl-phosphinate

ABSTRACT

A flame retardant additive, aluminum poly-hexamethylenephosphinate (APHP) with a polymeric structure was synthesized from 1,5-hexadiene, hypophosphorous acid and aluminum ions. The molecular structure of APHP and thermal stability were characterized by solid nuclear magnetic resonance, Fourier transform infrared and thermogravimetric analysis. Then, APHP was applied into diglycidyl ether of bisphenol-A cured by 4,4′-diamino-diphenylmethane. APHP showed flame-retardant effect on the epoxy thermosets in limited oxygen index (LOI), UL94 vertical test and cone calorimeter. The thermosets with only 4 wt.% APHP obtained an LOI value of 32.7% and reached the UL94 V-1 rating. The APHP/EP thermosets decreased the pk-HRR, THR and av-EHC values, decreased CO_2Y and enhanced the COY ratios, and also reserved more residual char comparing with neat thermoset. The less incorporation of APHP in thermosets will impose the better flame retardancy to epoxy thermosets. The flame-retardant effect of APHP was resulted by its two main pyrolyzed contents phosphorus and alkyl-phosphinic fragments. In condensed phase, the phosphorus-containing contents facilitated to the higher char yields and the formation of intumescent char layer, which led to a reduction of the released fuel and a strong barrier effect to weaken the combustion intensity. In gas phase, the PO, PO_2 and alkyl-phosphinic fragments with quenching effect were released from the phosphorus-containing contents, and can decrease the heat release and weaken the combustion intensity.

1. Introduction

In the recent years, high-performance halogen-free flame-retardant systems have become one of the most noteworthy topics in flame retardant fields to avoid the environment problems of several halogen-containing flame retardants [1]. Phosphorus-based flame retardants like phosphaphenanthrene, phosphazene, phosphate and phosphinate were all considered as effective contents to most of polymers [2,3]. Due to outstanding flame-retardant effect and water resistance, alkyl-substituted phosphinates were especially taken more attention in both commercial application and scientific research [4].

Alkyl-substituted phosphinates were first prepared and commercialized by Clariant Co. Series of metal alkyl-substituted phosphinates, especially aluminum salt of diethylphosphinic acid (AlPi), have been designed, synthesized and applied [5–9]. It is reported that AlPi and its composites are commercially available as Exolit OP1230, 1240, 1312, 1200, 1311 [10–14]. AlPi was found to be well working in polyamides and glass fiber reinforced polyamides, poly(ethylene terephthalate) and poly(butylene terephthalate) [4,15–18], also in poly(methyl methacrylate), polyurethane, and polyolefin [19–22]. In addition, some other kinds of alkyl-substituted phosphinates, e.g. aluminum diisobutylphosphinate and aluminum phenylphosphinate, were also proven to be effectively flame retardant in some certain polymer composites [23–25]. Polyamides and polyesters system were most researched in the flame-retardant application of AlPi. Ramani et al. investigated the flame-retardant mechanism of AlPi in combination with melamine polyphosphate and organically modified montmorillonite nanoclay in PA6 [26]. Schartel et al. applied AlPi in synergize with melamine polyphosphate and zinc borate in glass-fiber-reinforced PA66 and found that the AlPi acted mainly by flame inhibition [10]. Horrocks et al. investigated the combined effects and

* Corresponding author. Zonghe Building No.403, Fucheng Road NO.33, Haidian District, Beijing, PR China.
E-mail address: qianlj@th.btbu.edu.cn (L. Qian).

http://dx.doi.org/10.1016/j.polymdegradstab.2015.10.011
0141-3910/

burning behavior of AlPi and zinc stannate on HTPA [12]. Hao et al. found the synergistic effect between nano-Sb_2O_3 and AlPi on the flame retardancy of PET [27]. Gallo et al. investigated the flame retardancy of PBT containing AlPi and nanometric metal oxides and found that AlPi acted mainly in the gas phase through the release of diethylphosphnic acid [28].

In addition, studies on alkyl-substituted phosphinates with similar structure to AlPi have been further investigated. While the alkyl-substituted phosphinates change their metal type and structure of the alkyl groups, they will cause different flame-retardant effect on polymers. Wang et al. investigated that the mixture of diisobutylphosphinic and monoisobutylphosphinic aluminums were found to be effective on glass fiber reinforced PA6 [23,24]. Fang et al. prepared cerium phenylphosphonate and found low synergistic flame-retardant effect with decabromodiphenyl oxide in glass-fiber reinforced PET [29]. Liu et al. prepared zinc methylethylphosphinate and applied it into epoxy thermoset (EP) [30].

Normally, the phosphorus-based flame retardants can endow EP well flame retardancy [31], such as the aromatic phosphates [32], phosphaphenanthrene [33–35], cyclotriphosphazene [36], phosphorus-containing silsesquioxane [37], pentaerythritol diphosphonate [38,39]. The flame retardant application of alkyl-substituted phosphinate were seldom reported in the previous literature.

To further explore the influencing rule on flame retardancy of different molecular structures of alkane in alkyl-substituted phosphinates, the alkyl-substituted phosphinates was attempted to be constructed to a polymeric macromolecule. According to this assumption, a flame retardant additive, aluminum polyhexamethylenephosphinate (APHP) with a polymeric structure, was synthesized and characterized. The flame retardancy, the pyrolysis route and flame-retardant mechanism of APHP in epoxy thermosets were also investigated.

2. Experimental

2.1. Materials

1,5-hexadiene was purchased from Tokyo Chemical Industry Co. Ltd., Japan. The diglycidyl ether of bisphenol-A (commercial name: E-51), was obtained from Blue Star New Chemical Material Co. Ltd., China. Hypophosphorous acid, aluminum chloride hexahydrate, 4,4′-diamino-diphenylmethane (DDM), 2,2′-azobis(2-methylpropionitrile), and propanol were purchased from Sinopharm Chemical Reagent Co. Ltd.

2.2. Synthesis of APHP

Hypophosphorous acid (50% wt.% H_2O) (137.3 g, 1.04 mol) was melted in propanol(350.0 g, 5.83 mol) with mechanical stirring in a three-neck flask. Then 1,5-hexadiene (65.6 g, 0.80 mol) was added into the mixed solution with reflux condensing, and 2,2′-azobis(2-methylpropionitrile) (1.3 g, 0.008 mol) was added into the reaction system as initiator. The reaction temperature was then elevated to 65 °C within 20 min, and the mixture was stirred for 24 h. While the mixture turn to white emulsion, aluminum chloride hexahydrate (83.6 g, 0.35 mol) dispersed in 100 mL propanol was dripped into the reaction system within 60 min. After another 16 h, more white granules appeared. The resulting solids were then filtered off. The solids were washed and filtrated with water at 80 °C till the PH value of the filtrate was 7. The reaction formula is shown in Scheme 1. Finally the products were dried at 120 °C and the yields was >92.0%. FT-IR (KBr, cm^{-1}): 2924 and 2857 (C–H); 2356 (P–H); 1459 and 1405 (P–CH_2); 1176 (P=O); 1093 (P–O); 716 (P–C). ^{1}H NMR (ppm): δ = 2.29 (C–H), δ = 4.51 (P–H); ^{13}C NMR: δ = 31.54 (–CH_2–**C**H_2–CH_2), 22.82 (CH_2–**C**H_2–PO_2–); ^{31}P NMR (ppm): δ = 37.54 (–$(CH_2)_6$–PO_2^-–$(CH_2)_6$–), 18.98 (–$(CH_2)_6$–PO_2–H); ^{27}Al NMR (ppm): δ = 13.61. Phosphorus content: 20.3 wt.%.

2.3. Preparation of flame-retardant EP and the control sample

DGEBA and APHP were heated to 120 °C and stirred till APHP was completely dispersed in DGEBA. DDM was then added into the mixture at 110 °C and blended thoroughly. After the mixture was degassed at 120 °C for 3 min, it was poured into the preheated molds and cured at 120 °C for 2 h and then at 170 °C for 4 h. The samples were labeled as 1%APHP/EP, 2%APHP/EP, 3%APHP/EP, 4% APHP/EP and 6%APHP/EP based on the mass fraction of APHP in EP thermosets. The control sample, EP, was also prepared in the same manner but without the addition of the flame retardant APHP. The formulas of DGEBA, DDM, and APHP in each epoxy thermosets are listed in Table 1.

2.4. Characterizations

FTIR spectra were obtained using a Nicolet iN10MX-type spectrometer. The powdered samples were thoroughly mixed with KBr and then pressed into pellets. The ^{1}H NMR, ^{13}C NMR, ^{27}Al NMR and ^{31}P NMR data were obtained using a Bruker 400 MHz WB Solid-State NMR Spectrometer.

The phosphorus content was detected using Perkin Elmer Optima 8000 inductively coupled plasma optical emission spectrometry (ICP-OES).

Thermogravimetric analysis (TGA) was performed using a TA instrument Q5000 IR thermal gravimetric analyzer. The sample was placed in an alumina crucible and heated from 50 °C to 700 °C at the rate of 20 °C/min in N_2 atmosphere. All the tests were repeated three times, and the typical TGA data were reproducible within ±5%.

To detect volatile pyrolysis products, a Mettler-Toledo TGA/DSC-1 thermogravimetric analyzer was coupled to a Bruker Tensor 27 Fourier-transform infrared spectrometer (TGA-FTIR). Each sample was placed in an alumina crucible and heated from 50 to 700 °C at a heating rate of 20 °C/min under N_2 atmosphere. The thermogravimetric analyzer and FTIR spectrometer were connected by a quartz capillary at 230 °C.

The limited oxygen index (LOI) value was measured using an FTT (Fire Testing Technology, UK) Dynisco LOI instrument according to ASTM D2863-97 (sample dimension: 130.0 mm × 6.5 mm × 3.2 mm). The vertical burning test for the UL 94 combustion level was performed using an FTT0082 instrument according to ASTM D 3801 (sample dimension: 125.0 mm × 12.7 mm × 3.2 mm). The cone calorimeter test was performed using an FTT0007 cone calorimeter according to ISO5660 at an external heat flux of 50 kW/m^2 (sample dimension: 100 mm × 100 mm × 3 mm). The measurement for each specimen was repeated three times, and the error values of the typical cone calorimeter data were reproducible within ±10%.

The micromorphology images of the residues after cone calorimeter test were obtained using a FEI Quanta 250 FEG field-emission scanning electron microscope at high vacuum conditions with a voltage of 30 kV. The element contents of residues from cone calorimeter test were investigated via an AMETEK Quanta 250 FEG/EDS Energy Dispersive Spectrometer. The tested specimens were obtained from the surface of residues with sufficiently mixed and grinded, and the results were the average of the three times repeated tests which were all reproducible within ±5%.

To recognize the pyrolysis fragments of APHP, a Shimadzu GC-MS-QP5050A gas chromatography-mass spectrometer equipped with a PYR-4A pyrolyzer was employed. The helium (He) was

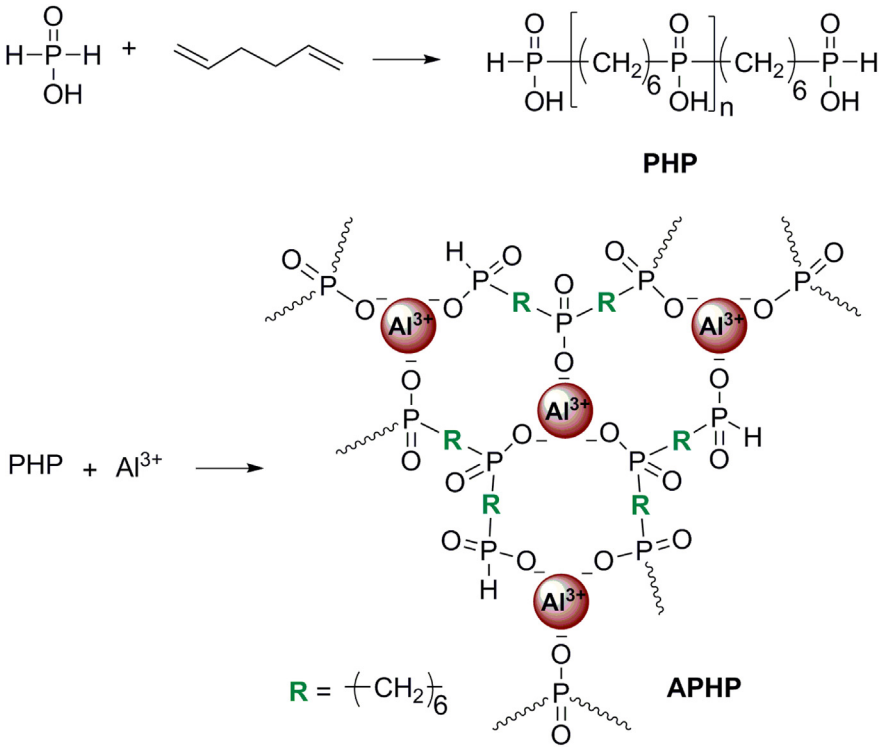

Scheme 1. Synthesis route of APHP.

utilized as carrier gas for the volatile products. The injector temperature was 250 °C, the temperature of GC/MS interface was 280 °C and the cracker temperature was 550 °C.

3. Results and discussion

3.1. Characterization of the molecular structure of APHP

As a macromolecule, the molecular weight of APHP is distributed in a certain scope. Due to the excess addition of hypophosphorous acid during synthesis process of APHP, the polymerization degree of APHP is small and the hypophosphorous acid substituted by single hexamethylene became end group. According to the synthesis character of APHP, its structure is confirmed in the subsequent discussion. Fig. 1 presents the ^{1}H NMR, ^{13}C NMR, ^{31}P NMR and ^{27}Al NMR spectra of APHP sample. In Fig. 1(a), the ^{1}H NMR spectrum exhibits a main strong absorption at 2.29 ppm, which is assigned to C–H bond of hexamethylene group. Another weak absorption at 4.51 ppm should be caused by P–H bond in the spectrum, whose absorption intensity is much weaker than that of the C–H bond. The existence of P–H absorption implies that one of two P–H bonds in hypophosphorous acid did not react with 1,5-hexadiene and were reserved as end groups of APHP. In Fig. 1(b), the two absorption bonds at 31.54 ppm and 22.82 ppm in the ^{13}C NMR spectra are assigned to the $-CH_2-CH_2-CH_2$ and $CH_2-CH_2-PO_2-$ groups respectively, and the ratio (1.00:0.49) of the relative integral area of two absorption peaks was approximately corresponded with the quantity ratio of two kind of carbon atoms in APHP molecule. In Fig. 1(c), the ^{31}P NMR spectra gives two absorption at 37.54 ppm and 18.98 ppm, which were caused by P atoms in C–P–C and C–P–H groups separately. The integral area ratio of the two peaks is 1.00/0.96. The ratio corresponds to that of P atom in C–P–C and C–P–H groups. The ^{31}P NMR result also is consistent with the data in ^{1}H NMR and ^{13}C NMR data above. The ^{31}P NMR, ^{1}H NMR and ^{13}C NMR results all demonstrate that the main molecular chain of APHP were most likely to be a structure as $HPO_2-(CH_2)_6-PO_2-(CH_2)_6-PO_2-(CH_2)_6-HPO_2-$, which possesses two kinds of phosphorus atoms, two kinds of carbon atoms and two kinds of hydrogen atoms. In Fig. 1(d), the single strong peak at −13.81 ppm can be attributed to the aluminum atoms in a same chemical environment, which proves that no inorganic aluminum hypophosphite existed in the resulting products. From all the above, these NMR data can demonstrate that the APHP was successfully synthesized. Furthermore, the high thermal stability of APHP sample detected by the following TGA test and the subsequent MS results of pyrolyzed fragments also confirmed the successful synthesis of APHP from another view.

Table 1
Formulation of the EP thermosets.

Samples	DGEBA (g)	DDM (g)	APHP		P-content (wt.%)
			(g)	(wt.%)	
EP	100.0	25.3	–	–	0
1%APHP/EP	100.0	25.3	1.3	1.0	0.203%
2%APHP/EP	100.0	25.3	2.6	2.0	0.406%
3%APHP/EP	100.0	25.3	3.9	3.0	0.609%
4%APHP/EP	100.0	25.3	5.2	4.0	0.812%
6%APHP/EP	100.0	25.3	8.0	6.0	1.218%

3.2. Flame-retardant behaviors in EP thermosets

3.2.1. LOI and UL94 vertical tests

After the structure of APHP was confirmed, APHP was incorporated into EP thermosets for flame retardancy. The flame retardancy of the EP thermosets was detected using LOI and UL94 vertical burning tests first. The corresponding results are presented in Table 2. The LOI value of the neat EP sample was only 26.0%,

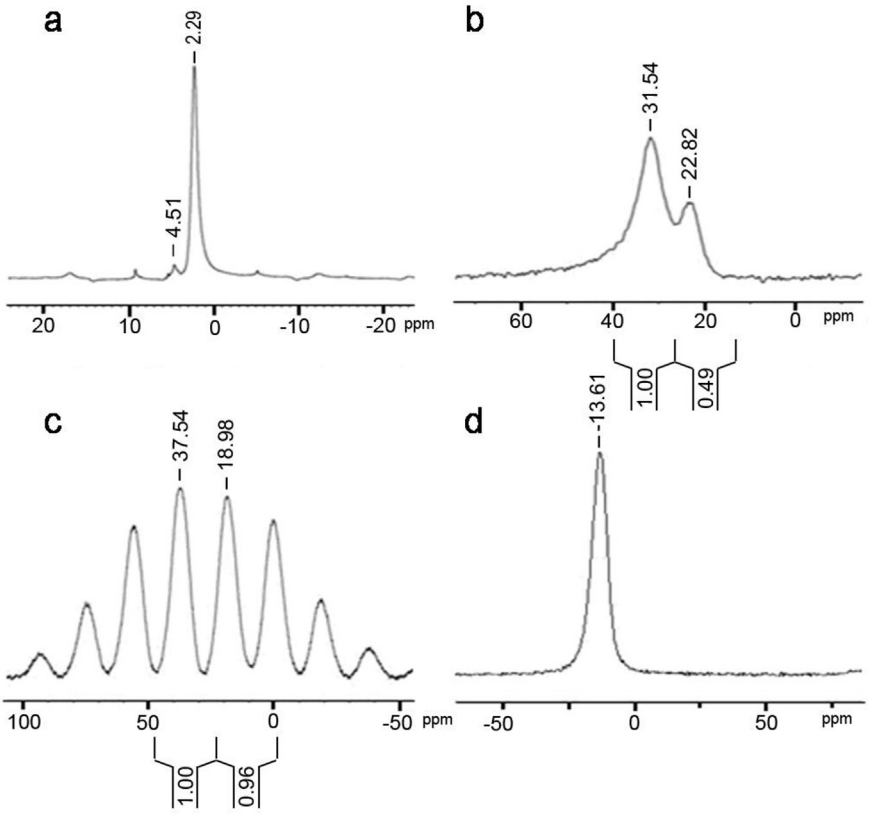

Fig. 1. (a) ^{1}H NMR; (b) ^{13}C NMR; (c) ^{31}P NMR; (d) ^{27}Al NMR spectra of APHP.

whereas the LOI value of 4%APHP/EP sample dramatically increased to 32.4%. The LOI values of the specimens can be further increased with increasing the mass ratio of APHP in the thermosets. The remarkable character is that the lower APHP loadings imposed the high LOI value to the flame-retardant thermosets. Accompanying with LOI results, the UL94 vertical burning test of thermosets containing APHP also exhibited different flame-retardant rule.

The UL94 vertical burning test results indicate that the neat EP thermosets sample cannot be rated according to the UL94 rule because its av-t_1 value reached to142 s and did not flame out after the second ignition accompanying with dripping during combustion. The UL94 ratings of the EP thermosets were enhanced with increasing the mass fraction of APHP. When the mass fraction of APHP in thermosets reached 1 wt.%, it hadn't any dripping and shorted burning time during the vertical burning test but it was also unrated. These phenomena disclosed the better anti-dripping properties of APHP. When the mass fraction of APHP increased to 4 wt.%, the 4%APHP/EP sample reached the UL94 V-1 rating with the shorter burning time and without dripping. But with further increasing mass ratio of APHP, the 6%APHP/EP sample with the higher LOI value didn't pass the UL94 test again.

Summing up the discussion on LOI and UL94 tests, APHP can endow thermosets with the higher LOI value and UL94 V-1 rating when the less APHP was incorporated into thermosets, which preliminarily revealed the flame-retardant action rule of APHP.

The flame-retardant effect of APHP should be resulted by the special chemical structure (i.e. aluminum alkyl-phosphinate) although the structure was linked together to form polymeric macromolecule. The aluminum alkyl-phosphinates have been researched for several years and the flame-retardant action and mechanism have also been detected [10,14,22,25], but the action mechanism of the kind of polymeric molecular structure is not explored. Therefore, the flame-retardant action mode of APHP in thermosets will be carefully elucidated in the subsequent discussion.

3.2.2. Cone calorimeter test

Cone calorimeter test was conducted to investigate sufficiently the flame-retardant behaviors of APHP in the EP thermosets. The testing time (600 s) of every specimen is same in the cone calorimeter. The curves of heat release rate (HRR) are shown in Fig. 2, and partial characteristic parameters, such as the time to ignition (TTI), peak of heat release rate (pk-HRR), residue yield, total mass loss (TML), average value of effective heat of combustion (av-EHC), total heat release (THR), average CO yield (av-COY), and average CO_2 yield (av-CO_2Y), are summarized in Table 3.

As shown in Fig. 2 and Table 3, the TTIs of the thermosets were hardly changed with the incorporation of APHP. According to the subsequent discussion on TGA data, the APHP molecules had a higher onset degradation temperature comparing with the EP thermosets, thereby not influencing on the TTIs of APHP/EP samples. With the development of the thermal degradation process,

Table 2
LOI value and UL94 rating of EP thermosets.

Samples	LOI (%)	UL-94			
		Rating	Dripping	av-t_1	av-t_2
EP	26.2	Unrated	Yes	142.0	infinite
1% APHP/EP	28.4	Unrated	No	42.1	40.1
2% APHP/EP	29.3	Unrated	No	34.5	14.8
3% APHP/EP	32.0	Unrated	No	24.8	18.7
4% APHP/EP	32.7	V-1	No	15.5	10.8
6% APHP/EP	33.1	Unrated	No	48.4	15.8

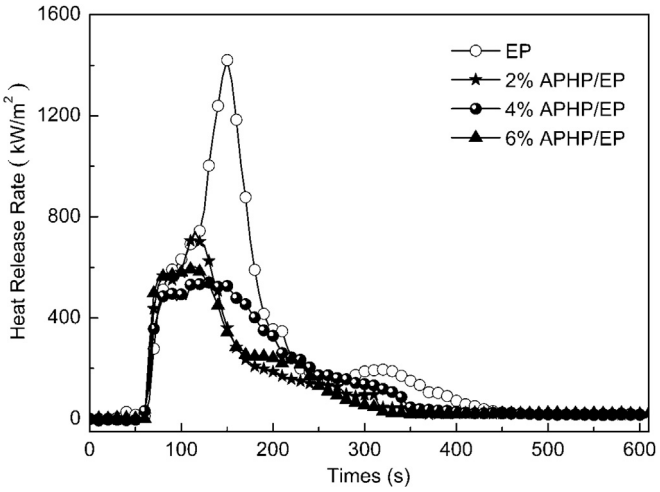

Fig. 2. Heat release rate curves of EP thermosets.

APHP began to decompose and work rapidly.

Another important parameter, TML, represents the total mass loss which is opposite to the residue yield in cone calorimeter test. And the residue yield can indicate the charring effect during combustion in cone calorimeter. In contrast to neat EP sample, the flame-retardant thermosets reduced the TML values with increasing APHP ratio in samples. But when adding 6% APHP into thermoset, TML value of 6%APHP/EP thermosets slightly decreased than that of 4%APHP/EP. Comparing with the neat EP, the TML value of the typical 4%APHP/EP decreased by 11.2%, which implies that more matrix formed residual char and decreased the release of flammable volatiles. Thus, APHP exhibits flame-retardant effect to some extent in condensed phase. Moreover, the HRR curves of neat EP was characterized by a sharp peak from the start to the end of burning, and this kind heat release characteristic is typical for non-charring materials [40]. However, all the APHP/EP thermosets with different dosages formed broad curves, which implies the flame retardant charring action in EP thermosets. The broadest curve from 4%APHP/EP should cause the highest residue yield. The result was confirmed by the residue yield data in Table 3.

THR values of the flame-retardant thermosets should also decrease due to the increase of char residue. Comparing with the neat EP sample, the THR of the 2%APHP/EP, 4%APHP/EP and 6% APHP/EP were decreased by 31.9%, 34.0% and 35.4%, respectively. The decrease in THR values were much larger than those of TML (7.7%, 11.2%, 9.6%). It disclosed that charring effect in condensed phase play a minor role in decreasing THR value.

What is the main role in decreasing THR value? It can be explained by av-EHC value, which discloses the burning degree of volatiles in gas phase during combustion. In Table 3, the av-EHC gradually decreased with increasing APHP contents, which clearly proves the existence of gas-phase flame-retardant effect of APHP. For example, about 26.4% decrease of av-EHC value in 4%APHP/EP sample revealed that the remarkable flame inhibition effect in gas-phase. More noteworthy, the gas-phase effect and charring effect in condensed-phase can be quantified by the reduction of EHC and the increase of residue yield [11]. For example, in 4% APHP/EP thermosets, the av-EHC value of EP was reduced to 73.6%(1−26.4%). The increased residue yield (16.5 wt.% instead 6.0 wt.%) reduced the amount of released fuel to 88.8% [(1−16.5%)/(1−6.0%)]. The tested THR value of 4%APHP/EP is reduced to 66.0%(1−34.0%), which accords to the calculated value well (THR calculated value: remaining EHC ratio × remaining fuel ratio = remaining THR ratio; 73.6% × 88.8% = 65.4%). Thus, comparing with the fuel reduction ratio (11.2%) resulted by the increased charring residue, the flame inhibition effect in gas-phase (26.4%) play a major role in the flame retardancy of APHP/EP thermosets.

The strong reduction in EHC can also explain the change in both COY and CO_2Y. As shown in Table 3, in contrast to the neat EP thermosets, the av-CO_2Y values of each APHP/EP thermosets decreased, which implies that the burning intensity were weakened. Whereas the av-COY did not change obviously while the av-CO_2Y decreased obviously. But the ratio of COY in contrast to CO_2Y obviously increased. The results are another evidence of APHP inhibiting effect on volatiles during combustion, thus resulting in more incomplete combustion products (CO) and less complete combustion products (CO_2). The reason of this behavior corresponded to that of the av-EHC decrease. It shows that the addition of APHP resulted in less released combustible volatiles and lower combustion intensity.

Further, the pk-HRR value of 4%APHP/EP thermosets show the lowest value, and decreased by 64.8% than that of neat EP thermoets. The pk-HRR decrease benefit from three ways: (1) the flame inhibition effect is represented by EHC; (2) the fuel reduction is represented by residue increase; (3) the barrier and protective effect of char layer need be calculated without the direct parameter [11]. Similar to the former quantitative assessment, the part reduction of pk-HRR originated from flame inhibition effect confirmed by the reserved av-EHC value 73.6% and the increased residue yield as determined by the reserved residue ratio 88.8%. The additional reduction of the pk-HRR was due to the protection effect caused by the intumescent charring residue, and the relative protection effect was calculated to be 46.7% (1−**53.3**%) (73.6% × 88.8% × **53.3**% = 35.2%). The strong barrier effect by the protective char layer decreased the pk-HRR value and weaken the intensity of combustion.

In 6%APHP/EP thermosets, the same quantitative assessment also can be taken. The reduction of the THR to 64.6% was attributed to the decreased EHC and the less fuel (71.6% × 90.4% = 64.7%). The pk-HRR was reduced to 42.5%. A reduction to 64.7% was assumed to be caused by the flame inhibition in gas phase and the increased charring residue. The additional reduction was due to the relative protection effect of the intumescent char layer of 34.3% (1−**65.7**%) (71.6% × 90.4% × **65.7**% = 42.5%). It obviously show that both the charring effect (9.6%) and the protection effect (34.3%) of the intumescent char decreased comparing with those of 4%APHP/EP sample. The deterioration in charring effect and barrier effect of intumescent char can also explain why 4%APHP/EP can pass V-1 rating, whereas 6%APHP/EP can not do.

Table 3
Typical parameters from cone calorimeter test of EP thermosets.

Samples	TTI (s)	THR (MJ/m^2)	pk-HRR (kW/m^2)	av-EHC (MJ/kg)	av-COY (kg/kg)	Residue (wt.%)	TML (wt.%)	av-CO_2Y (kg/kg)
EP	56	144	1420	29.9	0.13	6.0	94.0	2.51
2%APHP/EP	54	98	742	22.4	0.12	13.3	86.7	1.74
4%APHP/EP	58	95	540	22.0	0.12	16.5	83.5	1.75
6%APHP/EP	55	93	603	21.4	0.14	15.0	85.0	1.76

According to all the results, the thermosets with APHP were observed that 4% mass fraction of APHP was an appropriate ratio in thermosets, which can endow the thermosets with the better performance in both LOI test, UL 94 and cone calorimeter test.

3.3. TGA and TGA-FTIR analysis

The TGA curves of APHP are shown in Fig. 3, and some typical data are listed in Table 4. In Fig. 4, the onset degradation temperature ($T_{d,5\%}$) of APHP is 416 °C, which implies that APHP possessed the higher thermal stability than EP thermosets. Hence, at the initial thermal decomposition stage, all the curves from EP and APHP/EP thermosets coincided absolutely. It implies that APHP had no significant action on the initial decomposition of the APHP/EP thermosets. After the temperature rise, APHP began to decompose and worked on the EP matrix. The residual weight at 700 °C of the neat EP was about 14.1 wt.%, whereas the residual weight of APHP/EP at the same temperature were from 18.1 wt.% to 24.2 wt.% with increasing mass fraction of APHP. The increased residual weight ratio (4.0 wt.%–10.1 wt.%) resulted by the addition of APHP were more than the added mass fraction (2.0 wt.%–6.0 wt.%) of APHP in each APHP/EP thermosets. APHP showed the better charring effect on thermosets. This increase of char yields can be ascribed to the interaction between APHP and thermoset matrix, and the pyrolysis products of APHP promoted matrix charring.

The TGA-FTIR spectrum of APHP further discloses the pyrolysis process of APHP because that the main gas products of APHP from the thermal degradation process can be detected in Fig. 4(a) and (b). In Fig. 4(a), we can observe that the release rate of the decomposed gas gradually increased at about 1130 s and rapidly increased to a maximum value near 1300 s, then shortly gradually decreased till to the end. The gas release trend corresponded to the TGA result of APHP. We can calculate the relative accurate temperature of gas release by means of the combination of the TGA results and the TGA-FTIR 3D spectrum of APHP.

The FTIR spectrum of maximum gas release peak is shown in Fig. 4(b). The released gas information can be observed clearly. In this spectrum, the strongest broad peaks at 2937 cm^{-1} and 2956 cm^{-1} are responded to some alkyl and alkene groups coming from the pyrolysis hexamethylene of APHP. The peaks at 1652 cm^{-1}, 1457 cm^{-1}, 989 cm^{-1}, 949 cm^{-1} and 911 cm^{-1} provided the further evidence for the appearance of alkyl and alkene groups. The peak at 1250 cm^{-1} and 1170 cm^{-1} are attributed to PO_2 and PO absorption and the peak at 672 cm^{-1} is caused by P–C absorption. These phosphorus-containing group especially for PO_2 and PO with quenching effect can end the radicals. The results disclosed the flame-retardant effect of APHP in gas phase.

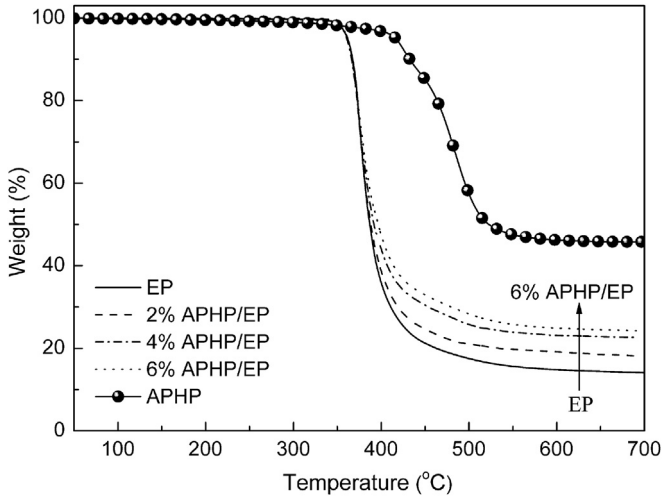

Fig. 3. TGA curves of APHP, neat EP, APHP/EP thermosets.

Table 4
TGA parameters of APHP, neat EP, APHP/EP thermosets.

Samples	$T_{d,5\%}$ (°C)	T_{max} (°C)	Residuals at 700 °C (wt.%)
Neat EP	361	376	14.1
2%APHP/EP	362	376	18.1
4%APHP/EP	361	375	22.9
6%APHP/EP	362	377	24.2
APHP	416	486	45.8

3.4. Morphology and element compositions of the residues from cone calorimeter test

3.4.1. Macroscopic and microscopic morphologies of residues

Fig. 5 shows the macroscopic digital images of the APHP/EP residues from cone calorimeter test. The residue from the neat EP sample was in a badly broken status with few amount, which implies the worse charring ability of EP itself. However, the residual char yields and expansion ratios of the other samples were elevated with the incorporation of APHP in thermosets. Comparing with the 6.0% char yield and the broken status of the EP residue, the 4% APHP/EP thermosets possessed 16.5% char yields and obviously expanded residual char morphology. APHP should not only increase the quantities of the residue but also elevate the expansion ratios of intumescent layer, thus resulting in strong protective effect of char layer.

To explore the flame-retardant charring mechanism further, SEM analysis was also carried out. Fig. 6 typically shows the residue SEM images of the EP and 4%APHP/EP samples from cone calorimeter test. The residue of neat EP sample shows many open holes with different sizes in Fig. 6(a). The open holes in the residue of EP sample provided channels for the combustible volatiles generated from the inner matrix to gas phase, and accordingly increasing the combustion intensity. Thus, complete combustion occurred. However, the residue of 4%APHP/EP sample in Fig. 6(b1) presents a sealed structure with a few obvious stretched tracks, which indicates the toughness enhancement of the thermoset melt during combustion. Fig. 6(b2) can demonstrate the opinion more directly in a higher magnification. As shown in Fig. 6(b2), the cotton-shaped cross-linking structure is continuous in the cracks of residue. The tougher and sealed residue of 4%APHP/EP sample can seal the combustible or incombustible volatiles generated by thermoset, and then cut off the fuel supply, and ultimately weaken the combustion intensity.

3.4.2. Elemental analysis of residues

Additionally, the element contents of the residue surface from the cone calorimeter tests were detected via Energy Dispersive Spectrometer (EDS). The results are shown in Table 5. The residue surface, which acted as the most direct connection to the air and heat radiation, had significant effect on the combustion in the cone calorimeter test. In Table 5, the phosphorus, aluminum and oxygen contents in all the residues remarkably rise with increasing mass fraction of APHP in thermosets. Differently, the carbon contents in all the residues turned to the opposite trend. The results imply that the surface char should be composed of the phosphorus oxides and aluminum phosphate combining with carbon compounds. The inflammable phosphorus oxides and aluminum phosphate contributed to forming an intumescent flame-retardant char layer, which inhibited the combustion process.

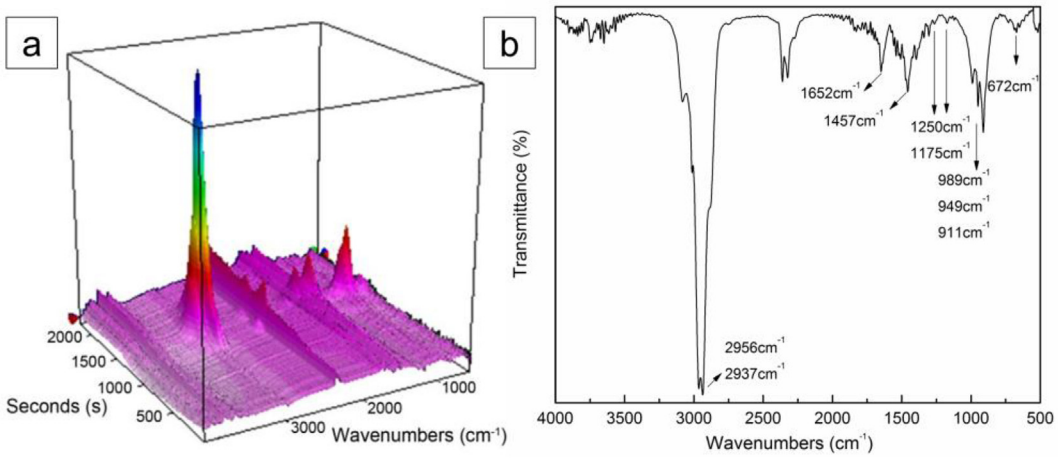

Fig. 4. (a) 3D FTIR spectrum of the pyrolysis gas products of APHP from TGA; (b) FTIR spectra of pyrolysis gas products of APHP at the maximum gas release rate.

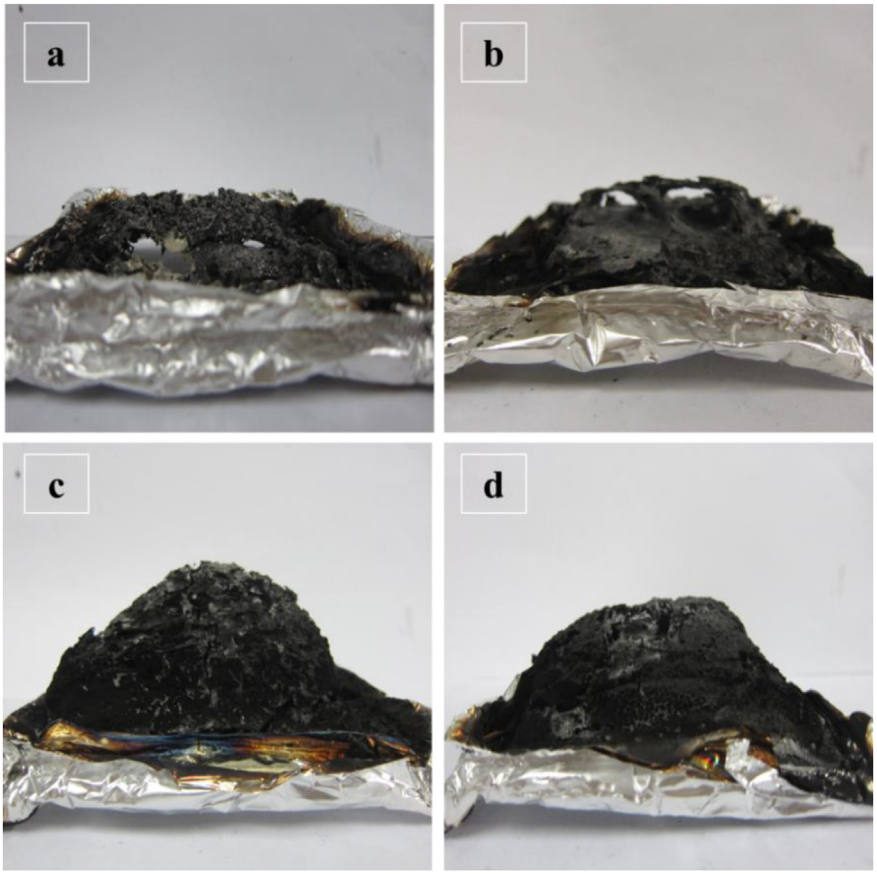

Fig. 5. Digital photos of thermoset residue from cone calorimeter. (a) EP; (b) 2%APHP/EP; (c) 4%APHP/EP; (d) 6%APHP/EP.

3.5. Flame-retardant mode and mechanism

3.5.1. Pyrolysis behavior of APHP

To further explore the pyrolysis behavior and its flame-retardant mechanism of APHP, the Py-GC-MS was adopted with a pyrolysis temperature at 550 °C. The GC spectrum of APHP is shown in Fig. 7. In Fig. 7, the pyrolysis fragments of APHP were mainly separated to three contents, whose retention times are 2.2 min, 7.7 min and 11.7 min, respectively. The contents between them were confirmed that they had similar molecular structures as that of the main three contents by means of analyzing their MS results. Therefore, to carefully analyze the chemical structures of the three main contents were adequate for exploring the flame retardant mechanism of APHP.

In accordance with the chemical structure of APHP shown in Scheme 1 and the typical *m*/*z* values provided in Fig. 8, the deduced pyrolysis route of APHP is illustrated in Fig. 9. In the pyrolysis route, APHP molecules were mainly decomposed into three kinds of fragments. In 2.2 min, the strongest fragment peak appears. It was formed by hexamethylene and its decomposed pieces, such as

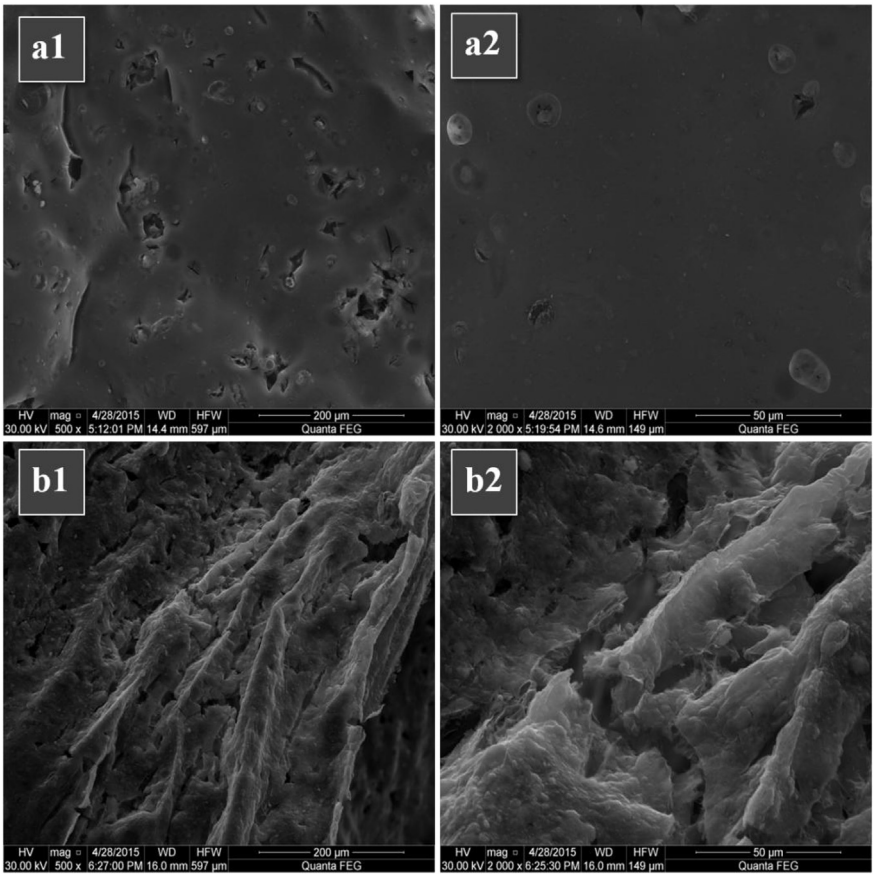

Fig. 6. SEM photos of the residues from cone calorimeter. (a) Pure EP, (a1-500×, a2-2000×) and (b) 4%APHP/EP, (b1-500×, b2-2000×).

Table 5
Element contents of residue surface from the cone calorimeter by EDS.

Samples	Element content (wt.%)				
	C	N	O	Al	P
EP	82.78	4.34	12.88	0	0
2%APHP/EP	74.85	9.37	13.78	0.58	1.42
4%APHP/EP	41.66	4.34	41.01	5.06	8.12
6%APHP/EP	39.99	3.80	40.58	5.08	10.55

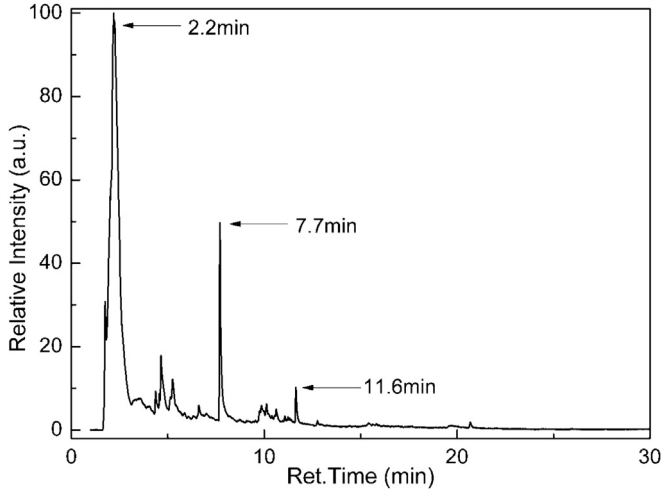

Fig. 7. GC spectrum of the pyrolysis products of APHP.

C_6H_{12} (hexadiene, $m/z = 84$), C_5H_{10} ($m/z = 70$), C_4H_8 ($m/z = 56$), $\cdot C_3H_5$ ($m/z = 41$). In 7.7 min, the appearance of the other strong peak was attributed to the phosphorus such as P_4 ($m/z = 124$), P_3 ($m/z = 93$), P_2 ($m/z = 62$). In the final, another typical peak was observed in 11.6 min, which can be caused by some fragments with more complex alkyl-phosphinic structure such as $-PO_2^- - C_6H_{11}$ ($m/z = 146$), $-PO_2^- - C_4H_6 -$ ($m/z = 117$),$-PO_2^- - C_3H_5$ ($m/z = 104$), and PO_2^- radicals ($m/z = 63$). Also some alkyl and alkene groups decomposed from alkyl-phosphinic structure, such as $\cdot C_6H_{13}$ ($m/z = 85$), $\cdot C_5H_7$ ($m/z = 67$), $\cdot C_4H_7$ ($m/z = 55$), $\cdot C_3H_5$ ($m/z = 41$), were

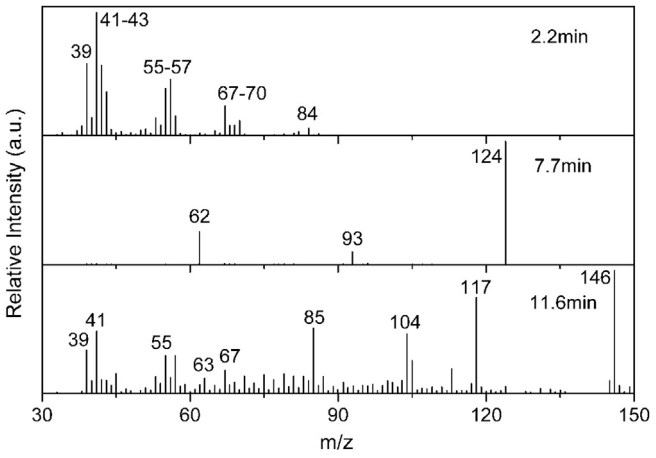

Fig. 8. MS spectra of main fragments of the pyrolyzed APHP at 550 °C.

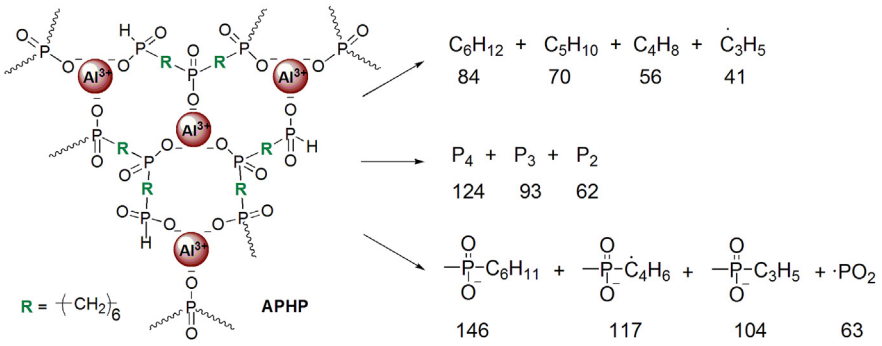

Fig. 9. The deduced pyrolysis route of APHP.

also observed. The fragments from the first peak in Fig. 8 do not contribute to the flame-retardant action, but the subsequence two stronger peaks can do it effectively.

3.5.2. *Flame-retardant mechanism of APHP in EP thermosets*

According to all the discussed results, the flame-retardant mechanism of APHP in EP thermosets is concluded in Fig. 10. After the thermosets was ignited, APHP was decomposed to alkyl-phosphinic structure and phosphorus, which can react and cross-link with the decomposed matrix. Accordingly, the flame-retardant phosphours-rich residue was formed. The pyrolyzed APHP also generated aluminum phosphate, which blended with phosphours-rich residue. The additional charring layer resulted in the reduction of fuel, and the intumescent residual char layer brought the barrier effect on fire and heat exchange, thereby resulting in condensed-phase flame-retardant effect. During combustion, APHP also released PO, PO_2 and alkyl-phosphinic pieces with quenching effect and exerted gas-phase flame-retardant effect. The quenching effect from PO, PO_2 and alkyl-phosphinic led to the flame inhibition effect in gas phase.

In sum, APHP exerts its flame retardant effect in three ways: (a) the charring effect decreased the fuel and resulted in the reduction of THR and pk-HRR; (b) the barrier and protective effects of the intumescent char layer weakened the intensity of combustion and resulted in the reduction of pk-HRR; (c) the flame inhibition from the pyrolysis pieces with quenching effect decreased both the THR and pk-HRR.

4. Conclusion

A polymeric flame retardant additive, aluminum polyhexamethylenephosphinate (APHP), was synthesized and applied in epoxy thermosets. The EP thermosets with only 4 wt.% APHP obtained an LOI value of 32.7% and reached the UL94 V-1 rating. The thermosets with APHP also decreased the pk-HRR, THR and EHC values, decreased CO_2Y amount and enhanced the COY ratio, and

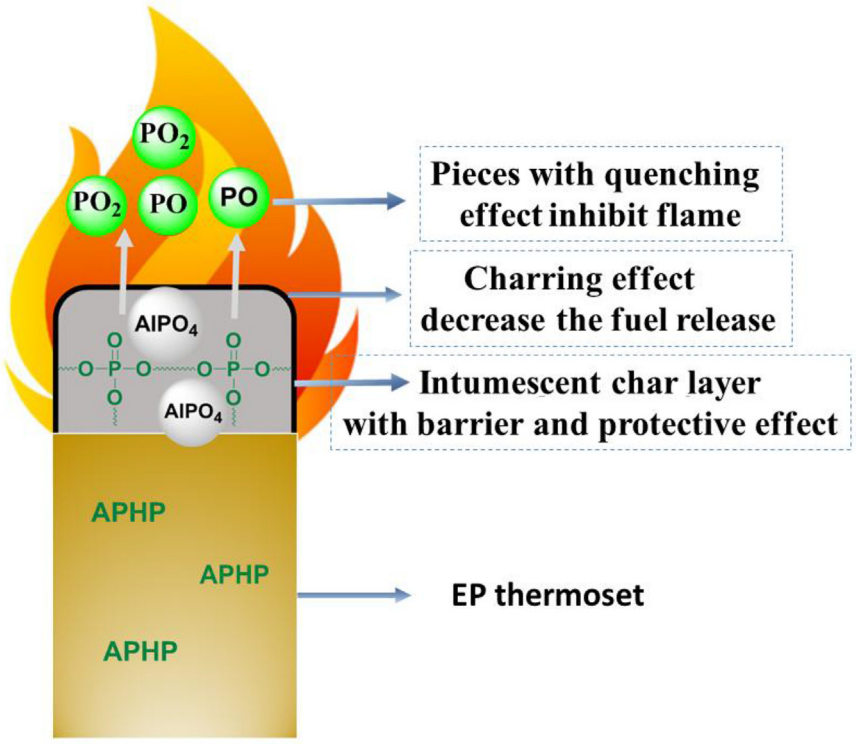

Fig. 10. Flame-retardant mechanism of APHP in EP thermosets.

also reserved more residual char comparing with neat thermoset. Therefore, the less addition of APHP in thermosets will impose the better flame retardancy to epoxy thermosets. The flame-retardant effect of APHP was generated by its two main pyrolyzed contents phosphorus and alkyl-phosphinic fragments. In condensed phase, the phosphorus-containing contents increased the residue yield. The more phosphorus-rich char blending with aluminum phosphate facilitated to the formation of intumescent char layer. The increased residue led to a reduction of the released fuel, and the intumescent char layer also resulted in a strong barrier effect to weaken the combustion intensity. In gas phase, the PO, PO_2 and alkyl-phosphinic with quenching effect were released from the phosphorus-containing contents, and can inhibit the flame and weaken the combustion intensity. Therefore, APHP conduct the flame retardant effect on epoxy thermosets both in condensed phase and gas phase.

Acknowledgments

Financial support was provided by key project of science and technology plan from Beijing Municipal Education Commission & Beijing Nature Science Foundations (No. KZ201510011009).

References

[1] I.V.D. Veen, J.D. Boer, Phosphorus flame retardants: properties, production, environmental occurrence, toxicity and analysis, Chemosphere 88 (10) (2012) 1119–1153.
[2] S.Y. Lu, I. Hamerton, Recent developments in the chemistry of halogen-free flame retardant polymers, Prog. Polym. Sci. 27 (8) (2002) 1661–1712.
[3] L. Chen, Y.Z. Wang, A review on flame retardant technology in China. Part I: development of flame retardants, Polym. Adv. Technol. 21 (1) (2010) 1–26.
[4] E. Schmitt, Phosphorus-based flame retardants for thermoplastics, Plast. Addit. Compd. 9 (3) (2007) 26–30.
[5] Hill M, Hoerold S, Krause W, Sicken M. Method for producing mixtures of alkylphosphonous acid salts and dialkylphosphinic acid salts: US 8889772.2014-11-18.
[6] Bauer H, Krause W, Sicken M, Weferling N. Dialkylphosphinic salts: US, 7420007. 2008-09-02.
[7] Weferling N, Schmitz HP, Kolbe G. Process for preparing salts of dialkylphosphinic acids: US, 6534673.2003-03-18.
[8] Schlosser E, Nass B, Wanzke W. Flame-retardant combination: US, 6255371. 2001-07-03.
[9] Jenewein E, Kleiner HJ, Wanzke W, Budzinsky W. Synergistic flame protection agent combination for thermo plastic polymers: US, 6365071. 2002-04-02.
[10] U. Braun, B. Schartel, M.A. Fichera, C. Jäger, Flame retardancy mechanisms of aluminum phosphinate in combination with melamine polyphosphate and zinc borate in glass-fibre reinforced polyamide 6,6, Polym. Degrad. Stab. 92 (8) (2007) 1528–1545.
[11] S. Brehme, B. Schartel, Fischer O. Goebbels, D. Pospiech, Y. Bykov, M. Döring, Phosphorus polyester versus aluminum phosphinate in poly(butylene terephthalate) (PBT): flame retardancy performance and mechanisms, Polym. Degrad. Stab. 96 (5) (2011) 875–884.
[12] A.R. Horrocks, G. Smart, S. Hörold, W. Wanzke, E. Schlosser, J. Williams, The combined effects of zinc stannate and aluminum diethylphosphinate on the burning behavior of glass fiber-reinforced, high temperature polyamide (HTPA), Polym. Degrad. Stab. 104 (2014) 95–103.
[13] A. Lorenzetti, M. Modesti, E. Gallo, B. Schartel, S. Besco, M. Roso, Synthesis of phosphinated polyurethane foams with improved fire behaviour, Polym. Degrad. Stab. 97 (11) (2012) 2364–2369.
[14] F. Samyn, S. Bourbigot, Thermal decomposition of flame retarded formulations PA6/aluminum phosphinate/melamine polyphosphate/organomodified clay: interactions between the constituents, Polym. Degrad. Stab. 97 (11) (2012) 2217–2230.
[15] C. Kaynak, O. Polat, Influences of nanoclays on the flame retardancy of fiber-filled and unfilled polyamide-6 with and without aluminum diethylphosphinate, J. Fire Sci. 33 (2) (2015) 87–112.
[16] Z.S. Zhan, M.J. Xu, B. Li, Synergistic effects of sepiolite on the flame retardant properties and thermal degradation behaviors of polyamide 66/aluminum diethylphosphinate composites, Polym. Degrad. Stab. 117 (2015) 66–74.
[17] X. Han, J.Q. Zhao, S.M. Liu, Y.C. Yuan, Flame retardancy mechanism of poly(butylene terephthalate)/aluminum diethylphosphinate composites with an epoxy-functional polysiloxane, RSC Adv. 4 (32) (2014) 16551–16560.
[18] U. Braun, H. Bahr, B. Schartel, Fire retardancy effect of aluminium phosphinate and melamine polyphosphate in glass fibre reinforced polyamide 6, E Polymers 10 (2010) 443–456.
[19] A. Laachachi, M. Cochez, E. Leroy, M. Ferriol, J.M. Lopez-Cuesta, Fire retardant systems in poly(methyl methacrylate): interactions between metal oxide nanoparticles and phosphinates, Polym. Degrad. Stab. 92 (1) (2007) 61–69.
[20] A. Lorenzetti, S. Besco, D. Hrelja, M. Roso, E. Gallo, B. Schartel, M. Modesti, Phosphinates and layered silicates in charring polymers: the flame retardancy action in polyurethane foams, Polym. Degrad. Stab. 98 (11) (2013) 2366–2374.
[21] H.X. Li, N.Y. Ning, L.Q. Zhang, Y.X. Wang, W.L. Liang, Different flame retardancy effects and mechanisms of aluminum phosphinate in PPO, TPU and PP, Polym. Degrad. Stab. 105 (2014) 86–95.
[22] K. Langfeld, A. Wilke, A. Sut, S. Greiser, B. Ulmer, V. Andrievici, P. Limbach, M. Bastian, B. Schartel, Halogen-free fire retardant styrene-ethylene-butylene-styrene-based thermoplastic elastomers using synergistic aluminum diethylphosphinate-based combinations, J. Fire Sci. 33 (2) (2015) 157–177.
[23] B. Zhao, L. Chen, J.W. Long, H.B. Chen, Y.Z. Wang, Aluminum hypophosphite versus alkyl-substituted phosphinate in polyamide 6: flame retardance, thermal degradation, and pyrolysis behavior, Ind. Eng. Chem. Res. 52 (8) (2013) 2875–2886.
[24] Z. Hu, L. Chen, G.P. Lin, Wang YZ. LuoY, Flame retardation of glass-fibre-reinforced polyamide 6 by a novel metal salt of alkylphosphinic acid, Polym. Degrad. Stab. 96 (9) (2011) 1538–1545.
[25] Z. Hu, G.P. Lin, L. Chen, Y.Z. Wang, Flame retardation of glass-fiber-reinforced polyamide 6 by combination of aluminum phenylphosphinate with melamine pyrophosphate, Polym. Adv. Technol. 22 (7) (2011) 1166–1173.
[26] A. Ramani, A.E. Dahoe, On flame retardancy in polycaprolactam composites by aluminum diethylphosphinate and melamine polyphosphate in conjunction with organically modified montmorillonite nanoclay, Polym. Degrad. Stab. 105 (2014) 1–11.
[27] M.M. Si, J. Feng, J.W. Hao, L.S. Xu, J.X. Du, Synergistic flame retardant effects and mechanisms of nano-Sb_2O_3 in combination with aluminum phosphinate in poly(ethylene terephthalate), Polym. Degrad. Stab. 100 (2014) 70–78.
[28] E. Gallo, U. Braun, B. Schartel, P. Russo, D. Acierno, Halogen-free flame retarded poly(butylene terephthalate)(PBT) using metal oxides/PBT nanocomposites in combination with aluminum phosphinate, Polym. Degrad. Stab. 94 (8) (2009) 1245–1253.
[29] C. Chen, Z.H. Guo, S.Y. Ran, Z.P. Fang, Synthesis of cerium phenylphosphonate and its synergistic flame retardant effect with decabromodiphenyl oxide in glass-fiber reinforced poly(ethylene terephthalate), Polym. Compos. 35 (3) (2014) 539–547.
[30] X.Q. Liu, J.Y. Liu, S. Sun, J. Chen, S.J. Cai, Novel flame-retardant epoxy based on zinc methylethyl phosphinate, Fire Mater. 39 (5) (2014) 599–608.
[31] S.V. Levchik, E.D. Weil, Thermal decomposition, combustion and flame-retardancy of epoxy resins – a review of the recent literature, Polym. Int. 53 (12) (2004) 1901–1929.
[32] W.D. Xiao, P.X. He, G.P. Hu, B.Q. He, Study on the flame retardance and thermal stability of the anhydride-cured epoxy resin flame retarded by triphenyl phosphate and hydrated alumina, J. Fire Sci. 19 (5) (2001) 369–377.
[33] L.J. Qian, Y. Qiu, N. Sun, M.L. Xu, G.Z. Xu, F. Xin, Y.J. Chen, Pyrolysis route of a novel flame retardant constructed by phosphaphenanthrene and triazine-trione groups and its flame-retardant effect on epoxy resin, Polym. Degrad. Stab. 107 (2014) 98–105.
[34] C. Klinkowski, S. Wagner, M. Ciesielski, M. Döring, Bridged phosphorylated diamines: synthesis, thermal stability and flame retarding properties in epoxy resins, Polym. Degrad. Stab. 106 (2014) 122–128.
[35] L.J. Qian, Y. Qiu, J. Liu, F. Xin, Y.J. Chen, The flame retardant group-synergistic-effect of a phosphaphenanthrene and triazine double-group compound in epoxy resin, J. Appl. Polym. Sci. 131 (3) (2014) 39709.
[36] L.J. Qian, L.J. Ye, G.Z. Xu, J. Liu, J.Q. Guo, The non-halogen flame retardant epoxy resin based on a novel compound with phosphaphenanthrene and cyclotriphosphazene double functional groups, Polym. Degrad. Stab. 96 (6) (2011) 1118–1124.
[37] W.C. Zhang, X.M. Li, R.J. Yang, Pyrolysis and fire behaviour of epoxy resin composites based on a phosphorus-containing polyhedral oligomeric silsesquioxane (DOPO-POSS), Polym. Degrad. Stab. 96 (10) (2011) 1821–1832.
[38] M. Gao, S.S. Yang, A novel intumescent flame-retardant epoxy resins system, J. Appl. Polym. Sci. 115 (4) (2010) 2346–2351.
[39] X. Wang, Y. Hu, L. Song, H.Y. Yang, W.Y. Xing, H.D. Lu, Synthesis and characterization of a DOPO-substitued organophosphorus oligomer and its application in flame retardant epoxy resins, Prog. Org. Coat. 71 (1) (2011) 72–82.
[40] B. Schartel, T.R. Hull, Development of fire-retarded materials-Interpretation of cone calorimeter data, Fire Mater. 5 (31) (2007) 327–354.